NASA TECHNICAL NOTE

NASA TN D-3433

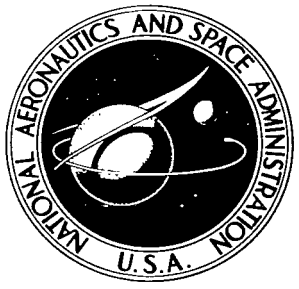

NASA TN D-3433

LOAN COPY: R
AFWL (W
KIRTLAND AF

TECH LIBRARY KAFB, NM

MANUAL CONTROL OF HIGH-ALTITUDE APOLLO LAUNCH ABORT

by Alfred J. Meintel, Jr., Kenneth R. Garren, and Norman R. Driscoll

Langley Research Center
Langley Station, Hampton, Va.

NATIONAL AERONAUTICS AND SPACE ADMINISTRATION • WASHINGTON, D. C. • JUNE 1966

TECH LIBRARY KAFB, NM
0130160

NASA TN D-3433

MANUAL CONTROL OF HIGH-ALTITUDE APOLLO LAUNCH ABORT

By Alfred J. Meintel, Jr., Kenneth R. Garren,
and Norman R. Driscoll

Langley Research Center
Langley Station, Hampton, Va.

NATIONAL AERONAUTICS AND SPACE ADMINISTRATION

For sale by the Clearinghouse for Federal Scientific and Technical Information
Springfield, Virginia 22151 – Price $2.00

MANUAL CONTROL OF HIGH-ALTITUDE APOLLO LAUNCH ABORT

By Alfred J. Meintel, Jr., Kenneth R. Garren,
and Norman R. Driscoll
Langley Research Center

SUMMARY

A fixed-base simulation study has been conducted to determine whether a pilot could manually orient the Apollo vehicle to the proper reentry attitude following a high-altitude (120 000 feet (36 576 m) and above) abort from earth launch by using only the "out-the-window" visual scene as an attitude reference. The effects of different visual scenes, vehicle control-system failures, and various aerodynamic characteristics caused by different launch vehicles and abort altitudes were investigated.

The results of over a thousand simulation runs show that manual orientation is possible but can be critical for certain abort conditions when control-system failures are present.

INTRODUCTION

The design of any U.S. manned space mission requires that the human occupants be able to abort the mission safely at any time events occur which could cause the loss of their life. The launch portion of the mission is a critical one for which this requirement exists. The Apollo launch escape system (LES) employs an escape tower attached to the manned spacecraft for the purpose of separating it from the Saturn launch vehicle in the event of a major malfunction. If an abort occurs during launch, the escape-tower rockets ignite and separate the spacecraft from the launch vehicle. However, the misalinements of the escape rockets cause the spacecraft—escape-tower combination to tumble randomly about all three axes after separation.

After the Apollo spacecraft has reached its maximum altitude and has started entry into a more dense atmosphere, it will orient itself into one of two possible aerodynamically stable attitudes. A trim attitude exists when either the apex (small end of the vehicle) or the heat shield (blunt end of the vehicle) is pointed forward. The apex-forward trim attitude is undesirable because excessive forces are exerted on the human occupants and the deployment of the landing parachute may be hampered. Therefore, a means must be provided to stabilize and orient the vehicle in a heat-shield-forward attitude. The method employed for this purpose is dependent upon the vehicle altitude at abort initiation (fig. 1).

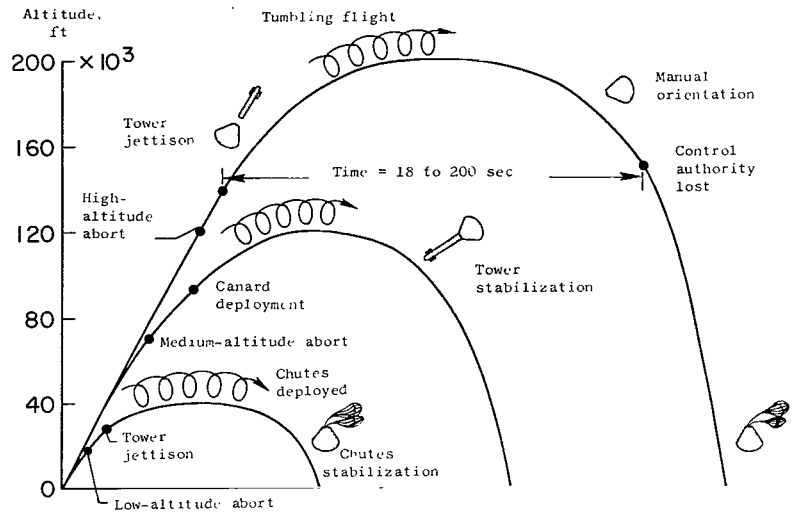

Figure 1.- Flight phases for Apollo launch aborts.

The low-altitude abort (launch pad to 25 000 feet (7620 m)) is fully automatic; the escape tower is jettisoned and the landing parachute is employed for vehicle stabilization. In the medium-altitude abort (25 000 to 120 000 feet (7620 to 36 576 m)), which is also automatic, the escape tower is retained and aerodynamic lifting surfaces (canard surfaces) at the upper end of the escape tower orient the vehicle into a heat-shield-forward attitude. In the high-altitude abort (120 000 feet (36 576 m) and above) the canard surfaces cannot be used for orientation because of the low air density at these altitudes. Thus, after LES burnout, the crew will manually jettison the escape tower and orient the vehicle to the desired reentry angle by using the attitude reaction control system (RCS) of the spacecraft.

The control time of 18 to 200 seconds shown in figure 1 is that time available in which the RCS of the vehicle can overcome the aerodynamic forces acting on the vehicle. This control time varies as a function of the altitude and velocity at which the abort was initiated.

A study conducted by North American Aviation, Space and Information Systems Division, Downey, California, showed that a pilot could perform the stabilization and orientation task by using the onboard attitude system of the spacecraft as a reference. However, the stable platform, which supplies the attitude information, might be unable to follow the vehicle rotations during the tumbling portion of the flight. Hence the onboard instrument reference would not be available for the orientation maneuver. If the instrument system were not functioning, the visual scene (through the spacecraft windows) would have to be used as a reference for determining the vehicle attitude.

The present report describes the results of a piloted simulation study in which the only reliable attitude information available was assumed to be the "out-the-window" visual

scene. The study was made to determine the ability of a pilot to orient the vehicle to the proper reentry angle (in the time available) by using the exterior visual scene, to develop an operational procedure for this orientation maneuver, and to determine the effect of malfunctions in the vehicle control system on the pilot's ability to perform the orientation task. Over a thousand simulation runs were conducted during the study, and the results of most of these are contained herein.

The authors would like to acknowledge Arthur G. Nolting of the Manned Spacecraft Center for his contribution of supplying the background information and aerodynamic data used in the study and Larry A. Bailey of North American Aviation, Inc., for his contribution of supplying the information on the Apollo vehicle systems used in the study.

SYMBOLS

The units used for the physical quantities defined in this paper are given both in the U.S. Customary Units and in the International System of Units (SI). Factors relating the two systems are given in reference 1.

a,b,c,d	quaternions
B	angle between top of window and X-axis of vehicle, degrees
C	depression angle of horizon, degrees
C_D	aerodynamic drag coefficient
C_L	aerodynamic lift coefficient
C_m	aerodynamic pitching-moment coefficient
E	orthogonal-transformation matrix
e_{ij}	element of E in ith row and jth column
F	force, pounds (newtons)
M	moment, foot-pounds (meter-newtons)
h	altitude, feet (meters)

I	moment of inertia, slug-foot^2 (kilogram-meter^2)
I_{sp}	specific impulse, seconds
l	aerodynamic reference length, feet (meters)
p	angular velocity about X-axis, radians/second
q	angular velocity about Y-axis, radians/second
$\bar{q}$	dynamic pressure, pounds/foot^2 (newtons/meter^2)
r	angular velocity about Z-axis, radians/second
S	aerodynamic reference area, feet^2 (meters^2)
s	distance along visual arc about local vertical, feet (meters)
t	time, seconds
V	relative velocity (tangential orbital), feet/second (meters/second)
W	weight of fuel, pounds (newtons)
X,Y,Z	Cartesian coordinates
α	angle of attack, degrees
β	sideslip angle, degrees
γ	relative flight-path angle, degrees
θ	pitch angle, degrees
φ	roll angle, degrees
ψ	yaw angle, degrees
Ω	angle about the local vertical, radians

ω	angular rate of visual-scene movement about the local vertical, degrees/second

Subscripts:

A	aerodynamic
B	body axis
cg	center of gravity
i	inertial axis
O	point of origin of body coordinate system
RCS	reaction control system
t	total
x,y,z	component for X-, Y-, or Z-axis

A dot over a symbol refers to the first derivative with respect to time. An arrowhead denotes positive direction.

EQUIPMENT

The equipment setup used in the study is shown in figure 2. The simulation program was conducted in a 53-foot-diameter (16-m) truncated sphere the interior of which was coated with a diffuse white paint. The white surface acted as a screen on which the visual scenes used in the study were projected. The pilot viewed the projected scene from a fixed-base Apollo command module mockup located near the center of the sphere. The scene was projected from a point-source light type of projector attached to the inner axis of a three-axis attitude drive system. The pilot controlled the position of the drive system by using a three-axis sidearm controller through an analog computer.

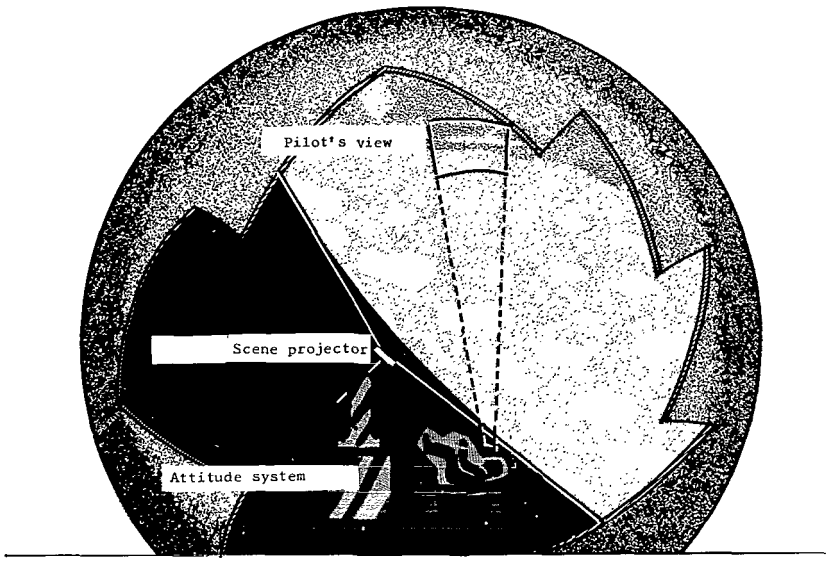

Figure 2.- Simulation facility.

ATTITUDE CONTROL

A schematic drawing of the roll-axis control system is shown in figure 3. Two different spacecraft attitude-control modes were simulated in the study: the stabilization-and-control-system (SCS) entry mode and the monitor mode. Selection of the control mode for all three axes was made by the pilot with a switch (switch 1 in fig. 3) on the instrument panel.

The simulated SCS entry mode was a proportional-rate-command system with rate and attitude feedback. The controller had three levels of output. When the controller was deflected out of detent, a signal was used to reset the attitude-error integrators to zero and hold them at that level until the controller was returned to detent. The attitude dead band was $\pm 2^{\circ}$ about the spacecraft attitude when the controller was released. Further deflection of the controller gave an output signal proportional to deflection. This output signal was compared with the rate feedback and the jets were actuated; the spacecraft was thus moved until the feedback rate was equal to the commanded rate within the dead band of $\pm 2^{\circ}$ per second. Maximum deflection of the controller actuated switches which controlled the jets directly. The maximum command rates when the controller was deflected to a point just before contact with the direct-command switch were 17° per second in roll and 5° per second in pitch and yaw.

The monitor mode was also a proportional-rate-command system with rate feedback. This mode provided no attitude hold. The rate dead band in this mode was

±0.2° per second and the maximum command rates were 0.5° per second in all axes. This mode also allowed direct control of the spacecraft jets by maximum controller deflection.

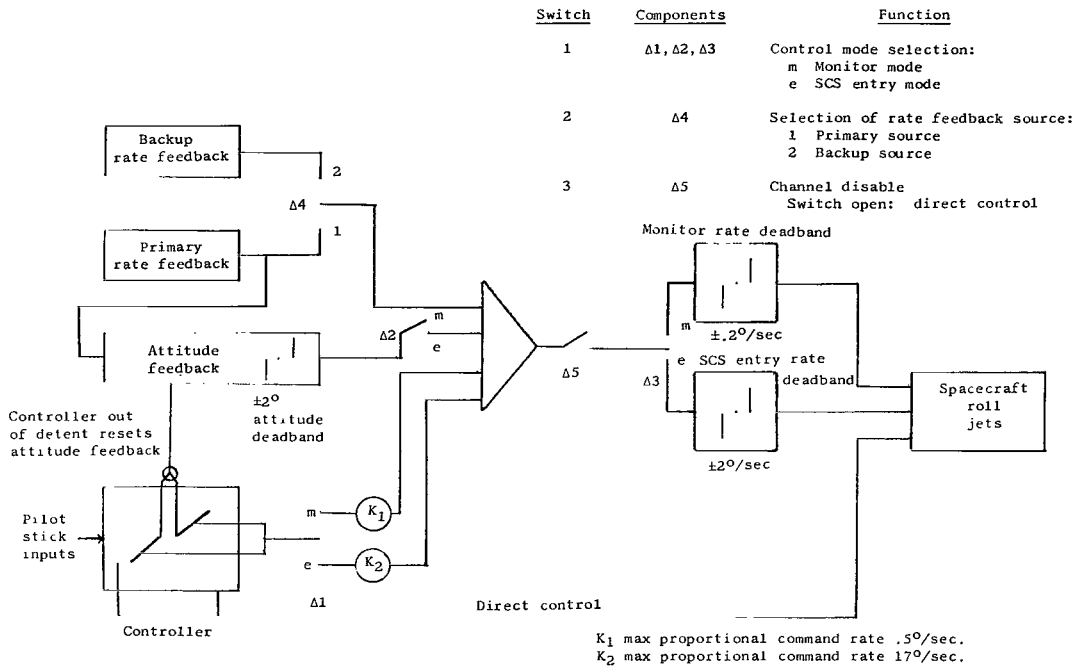

Figure 3.- Schematic drawing of control system for roll axis.

Six additional switches were located on the panel. Three of these switches (one for each axis) were used to disable the rate and attitude feedback (switch 3 in fig. 3). Actuation of this switch to the disable position (open) meant that maximum deflection of the controller was necessary to control spacecraft motions in the disabled axis. The remaining three switches selected primary or backup rate feedback for each axis (switch 2 in fig. 3). These switches were used to select backup rate when a failure was simulated in the primary rate feedback system.

The rate information was displayed to the pilot on a three-axis rate instrument on the panel. The maximum rate scaling was 20° per second in each axis. The rate instrument and switches are shown in figure 4.

VISUAL DISPLAY

The Apollo command module mockup used in the simulation provided the proper configuration and location of the command pilot's docking window and the left-hand side

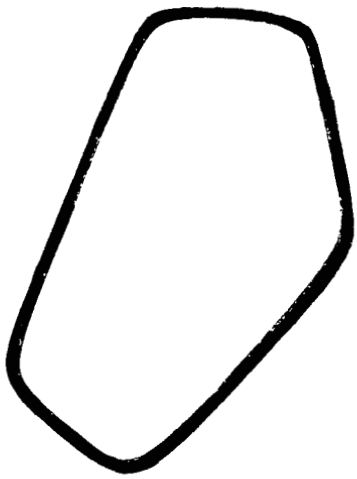

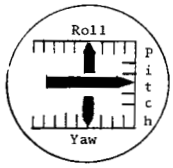

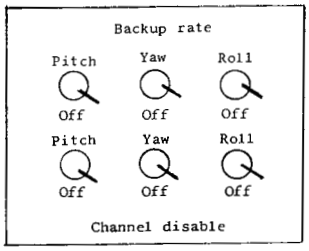

Figure 4.- Cockpit instrument display.

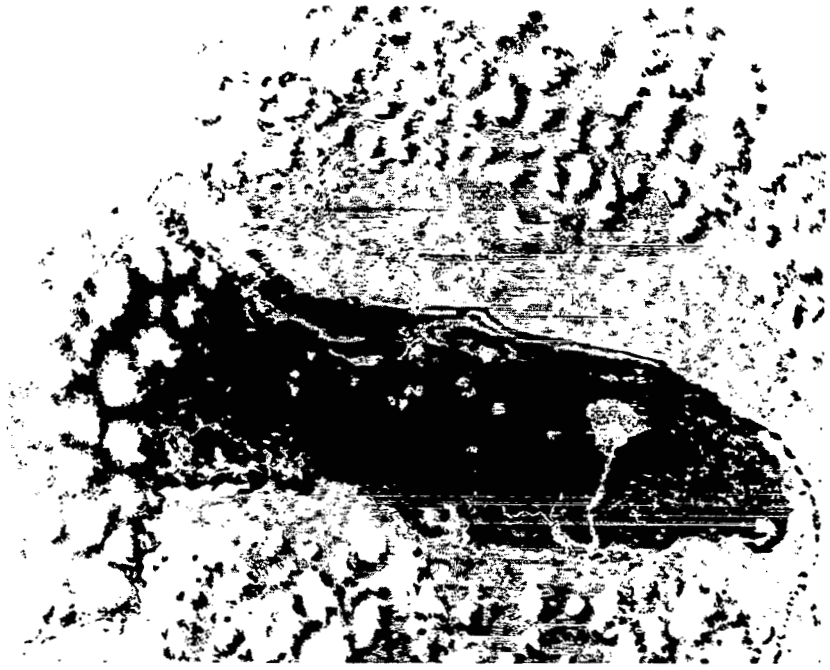

Figure 5.- Projection transparency of clear view of Florida. L-65-208

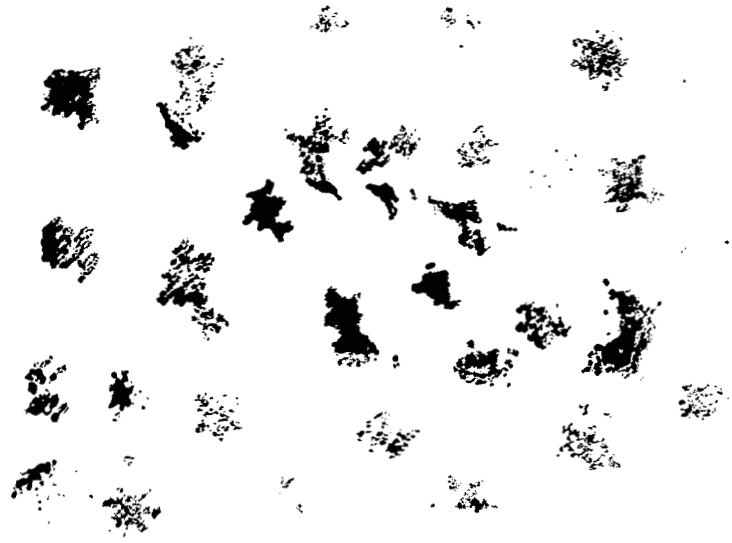

Figure 6.- Projection transparency of 90-percent-cloud-cover scene. L-66-1103

window. An Apollo-type couch was positioned so that the pilot eye position with respect to the windows was as it would be on the actual vehicle. The mockup also contained the hand controller, the rate instrument, and the switches discussed previously.

The only attitude reference used in the study was the out-the-window view. Three different scenes were used: A clear view of Florida with scattered clouds over the water (fig. 5); a 90-percent-cloud-cover scene with no recognizable landmark visible (fig. 6); and a 90-percent-cloud-cover scene in conjunction with a simulated rocket payload vapor trail (fig. 7). These scenes were projected over a 166.5° area by a point-source light projection system. An angle of 166.5° was required to present the entire view from horizon to horizon as seen from 167 000 feet (50 902 m). This altitude of the visual projection remained constant in all the simulations.

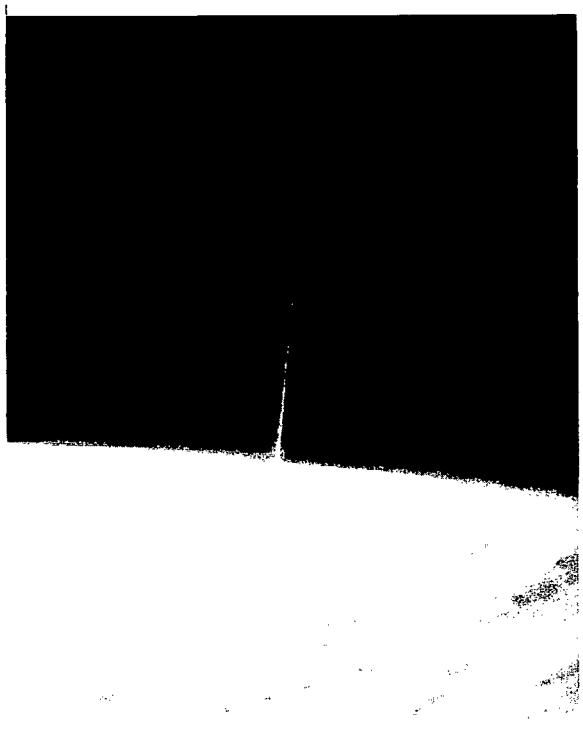

L-66-1133

Figure 7.- Projection transparency of 90-percent-cover scene with simulated vapor trail.

The projector for the land scenes consisted of the point-source light, a 20-inch-wide (0.51-m) transparency, and a servosystem to position the transparency. The point source, which was designed particularly for the simulation, was a 100-watt mercury arc lamp with its two ends bent into a V-shape (included angle of 120°). The lamp therefore gave a full hemispherical coverage of light of uniform intensity with no shadows. The transparency was made of 10-mil-thick (0.0003-m) plastic sheet on which was painted an artist's conception of Florida. Figures 5 and 6 are photographs of the actual transparencies used. These photographs are presented to show the amount of detail contained, but they are not representative of the view which the pilot had in the simulation. The light level of the simulated scene was one-thousandth of the actual brightness level. However, because of the excellence of the artist's conception, the resulting color contrast obtained, and the fact that projection was accomplished with a point source over a large angle (so that proper perspective was obtained), the view presented was very realistic in the pilot's opinion.

The projection of a 150-watt-filament lamp through a narrow slit simulated the payload vapor trail (fig. 7). The slit was covered with a Wratten No. 30 gelatin filter (orange-red) to simulate the release of sodium from the payload of a solid propellant rocket such as a Nike-Cajun. The sodium vapor trail subtended a 1^{o} angle in width and a 38^{o} angle in height.

The transparencies were positioned with respect to the point-source light by a position servosystem. The servosystem positioned the transparency so that the angular rate presented to the pilot was comparable to the rate at which the earth would appear to move in actual flight.

The projection box was mounted on the inner axis of the three-axis drive system. In the abort study, unlimited motion in all three axes was required. This freedom was accomplished by having no mechanical stops on the equipment and by operating the system with direct-coupled synchrodrives. The synchrodrives which positioned the attitude system were mounted on the front of the computer resolvers, and the shaft of the resolver was coupled to the shaft of the synchrodrive. The resolvers in the computer were operated in the "polar" computing mode, which allowed unlimited rotation in each axis. The equations used to compute the attitude are given in the appendix.

Simulation Procedure

The Apollo abort program was primarily a three-degrees-of-freedom simulation in which only angular rates and positions were involved. The aerodynamic rotational moments created by four different trajectories were programed into the simulation. These trajectories included those for both the Saturn IB and Saturn V launch vehicles with abort initiation at 120 000- and 150 000-foot (36 576- and 45 720-m) altitudes. The nonlinear aerodynamic parameters, shown in figure 8, were programed on diode function generators as a function of time from abort initiation. Shown in the figure are plots for the dynamic pressure $\bar{q}$, the vehicle flight-path angle γ, and the angular rate of motion of the visual scene ω as viewed from an orbiting vehicle along the local vertical. The integral of the rate ω was used to position the transparency with respect to the point-source light.

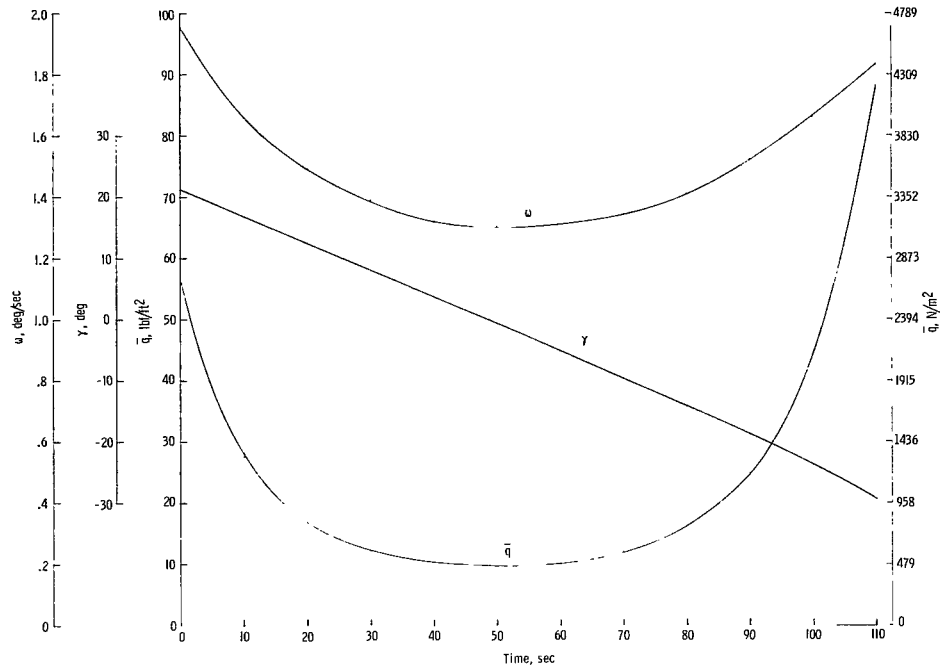

(a) Parameters for Saturn V 120 000-foot-altitude (36 576-m) abort.

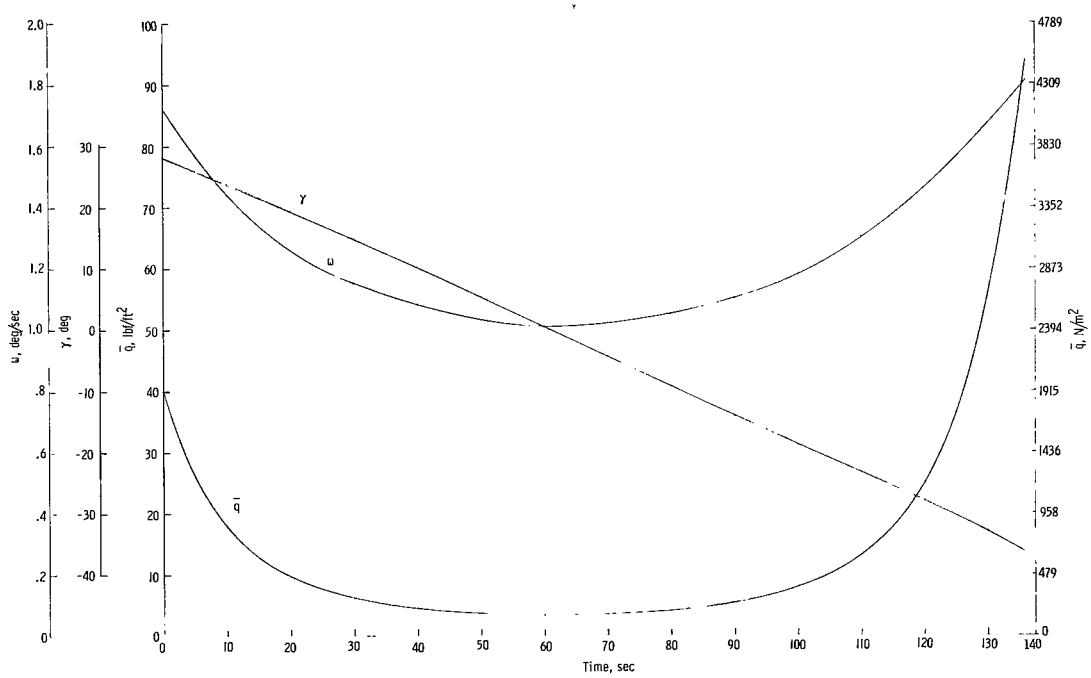

(b) Parameters for Saturn IB 120 000-foot-altitude (36 576-m) abort.

Figure 8.- Aerodynamic parameters programed as a function of time.

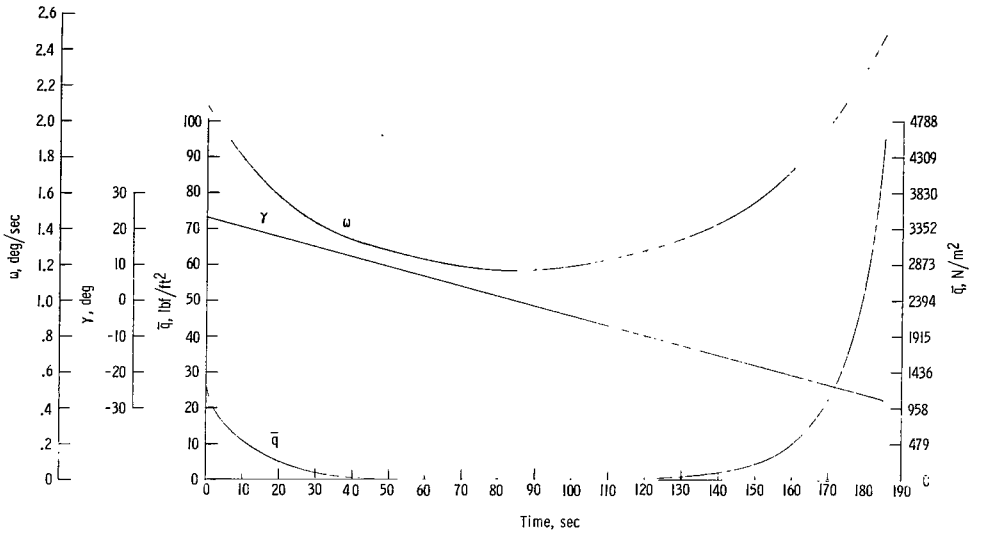

(c) Parameters for Saturn V 150 000-foot-altitude (45 720-m) abort.

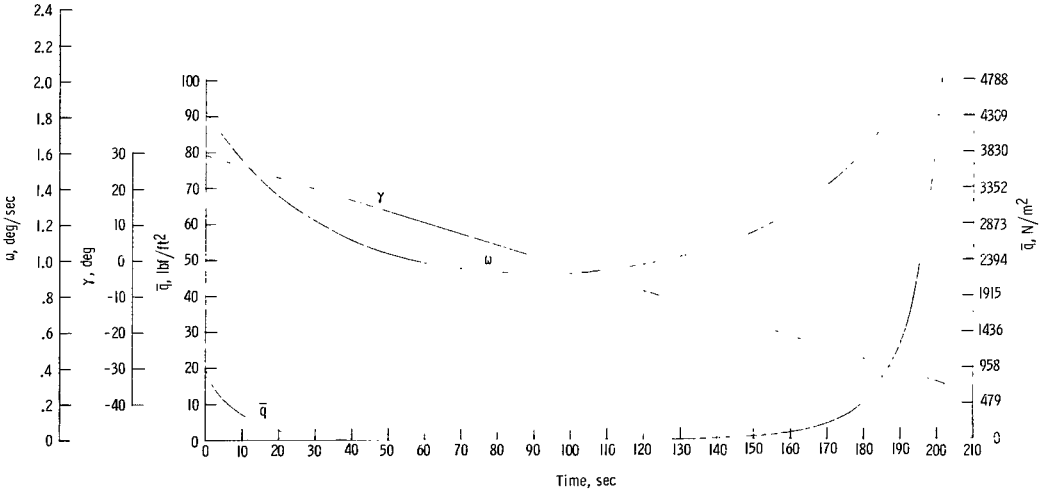

(d) Parameters for Saturn IB 150 000-foot-altitude (45 720-m) abort.

Figure 8.- Concluded.

The nonlinear aerodynamic coefficients C_D, C_L, and C_m were programed on diode function generators as a function of the angle of attack α of the spacecraft. The distribution of these coefficients was assumed to be symmetrical about the zero attitude position. Inasmuch as the center of gravity (c.g.) of the actual vehicle does not coincide with the centroid, the center-of-gravity offsets were programed in the equations of the appendix as constants. The resultant nondimensional moment coefficients as a function of the vehicle angles of attack and sideslip are given in figure 9.

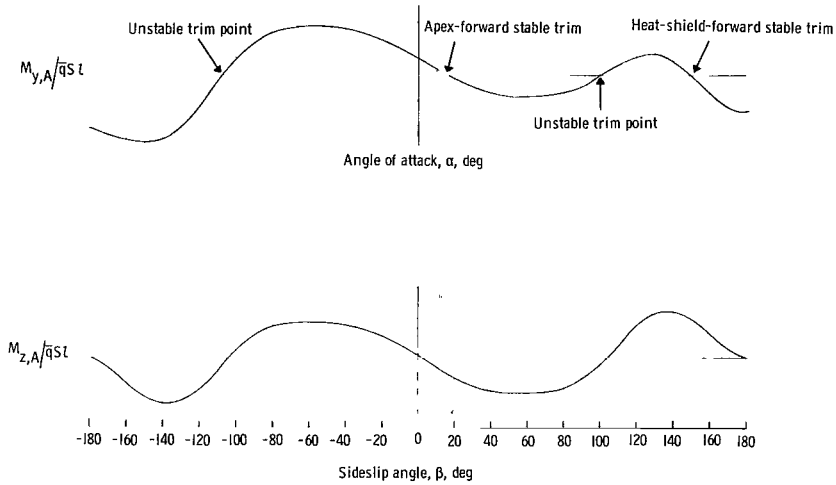

Figure 9.- Moment coefficients plotted as a function of vehicle angles of attack and sideslip.

The moment coefficient as a function of sideslip angle is plotted with the angles of attack and roll equal to zero; the moment coefficient as a function of angle of attack is plotted with the angles of yaw and roll equal to zero. The two stable and the two unstable trim attitudes of the vehicle are indicated.

The assumptions for the study were: (1) That the abort occurred and followed one of the four trajectories programed; (2) that the initial rotational rates during the tumbling phase of flight were 100° per second about each axis; (3) that the onboard attitude reference system gave unreliable information; and (4) that spacecraft rotational-rate information was presented on the cockpit instrument panel and also was available for use in the automatic-control-system feedback. Both single and dual RCS operation were used. In addition, various control-system failures were investigated. The pilot had a choice of the control system which would be used – either the monitor or the SCS entry mode.

It was further assumed that for all but one type of control-system failure, the tumble rates would be arrested by the automatic control system of the vehicle. Therefore,

most of the simulation runs started when the vehicle was at some fixed attitude in space and had rotational rates below the dead band of the control system. Table I shows a sketch of the vehicle axis system along with a list of the 25 initial conditions of attitude used in the study. The only runs for which the vehicle tumbling rates were not assumed to be zero were those in which control-system failures were investigated.

TABLE I.- INITIAL CONDITIONS OF ATTITUDE USED IN STUDY

Case	Yaw ψ, deg	Roll φ, deg	Pitch θ, deg
1	0	0	100
2	72	0	172
3	144	0	244
4	216	0	316
5	288	0	28
6	288	72	100
7	0	72	172
8	72	72	244
9	144	72	316
10	216	72	28
11	216	144	100
12	288	144	172
13	0	144	244
14	72	144	316
15	144	144	28
16	144	216	100
17	216	216	172
18	288	216	244
19	0	216	316
20	72	216	28
21	72	288	100
22	144	288	172
23	216	288	244
24	288	288	316
25	0	288	28

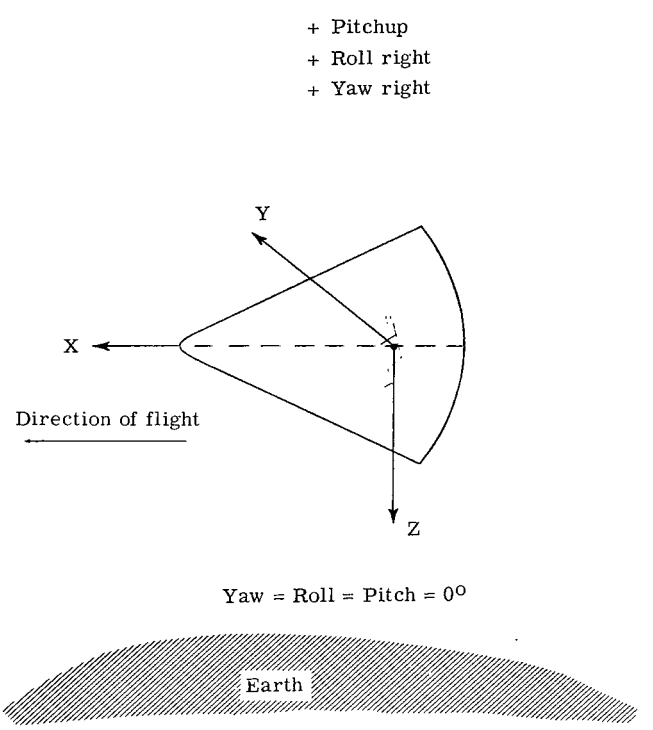

In addition to the main failure which caused the abort to occur, failures in the spacecraft reaction control system were investigated. One simulated failure was in the fuel (or jet) system and caused the loss of half the reaction control system. This failure was simulated (by the computer operator) by reducing the jet thrust to one-half the normal level before the pilot performed a run. The other failures investigated were in the feedback of the reaction control system (RCS). Four types of RCS failures were simulated with the stipulation that not more than one type of failure in only one axis would occur during the course of a piloted run. The four simulated malfunctions included spacecraft rate gyros open or closed and automatic-control-system switching amplifiers

open or closed. Table II gives the characteristics used for detection of each malfunction and the corrective actions required of the pilot.

TABLE II.- FAILURE PROCEDURE

Component	Failure	Detection cues	Corrective action
Rate gyro	Closed	Continuous acceleration in failed axis. Maximum deflection of failed-axis rate needle indicating motion in opposite direction to vehicle motion.	Disable failed axis. Manually damp rate in failed axis by using out-the-window scene. If rate needle still indicates rate, switch to backup rate gyro in failed axis. Enable axis.
Rate gyro	Open	Rate needle remains at zero during vehicle motion.	Manually damp rate. Switch to backup rate gyro in failed axis.
Switching amplifier	Closed	Continuous acceleration in failed axis detectable by rate-gage and out-the-window vision.	Disable failed axis. Manually damp failed-axis rate. Control in direct mode for remainder of run.
Switching amplifier	Open	No automatic rate damping in failed axis.	Manually damp failed-axis rate. Disable failed axis and control in direct mode for remainder of run.

The failures were simulated by the computer operator at various times during the run. The switching-amplifier-open failure simulation was initiated before the pilot took control. This failure caused the vehicle to continue tumbling about the failed axis while the automatic system damped the tumbling about the other two vehicle axes. This type of failure was simulated by starting the run at one of the 25 initial attitudes with a residual rate of 40^{o} to 60^{o} per second in the failed axis.

The run procedure was as follows: The initial conditions for the run were set on the computer by selecting the trajectory, the starting attitude of the vehicle, and the control system to be used (single or dual). The control mode (either monitor or SCS entry mode) was selected by the pilot before each run. The computer then positioned the equipment at the proper starting attitude. Upon a signal from the pilot, the computer was put into operation and the pilot was given control of the vehicle. During the run, the operator would insert a failure in the RCS if one was to be investigated in that run. The run was ended either when the pilot had oriented the vehicle to the proper attitude (to his satisfaction) and given a "hold" signal, or when the vehicle was aerodynamically captured. Aerodynamic capture, as defined in the present study, occurs when the dynamic pressure reaches a value above which the vehicle control power cannot pitch the vehicle in a pitchup direction from an apex-forward trim attitude to a heat-shield-forward trim attitude. This

value of dynamic pressure in the study was 20 lbf/ft^2 (958 N/m^2) for dual-control-system operation and 10 lbf/ft^2 (479 N/m^2) for single-control-system operation. The operator then read out the final conditions of the run. The readout consisted of the final attitude of vehicle, the time, and the fuel. In order to determine whether the vehicle was in the proper capture attitude (if in doubt), the computer was again put into operation and the dynamic pressure was allowed to increase to a value at which the spacecraft jets no longer had control. Then a final readout was obtained to determine whether the heat shield or the apex was forward at capture.

Pilot Procedure

The orientation of the pilot with respect to the earth during an abort is shown in figure 10. The launch is from Cape Kennedy, with an abort occurring at some altitude above 120 000 feet (36 576 m). The thrust misalinement of the escape-tower rockets cause the spacecraft-tower combination to tumble randomly. The pilot manually jettisons the escape tower and the spacecraft remains in the tumbling flight phase. The rate feedback from the onboard rate gyros will stop the tumbling if the system is operating properly. At this point the simulation runs are begun.

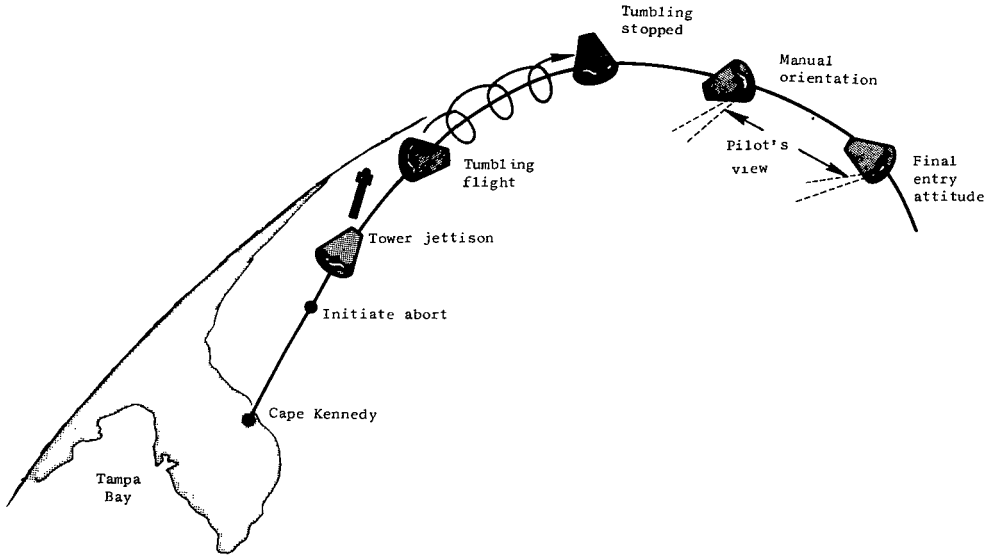

Figure 10.- Pilot orientation during Apollo launch abort.

The general procedure used by the pilots for each run is as follows:

(1) Check the rate needles and determine whether they are functioning properly (failure detection cues given in table II); null any existing rate in roll or yaw.

(2) If a pitch rate exists, allow it to continue until the earth scene appears in the window.

(3) If no pitch rate exists, pitch the vehicle up until scene appears.

(4) Maneuver the vehicle until proper heading (yaw attitude) is established. (The vehicle is at the proper attitude when the heat shield is in the direction of flight and the pilot is upside down with respect to the earth and is looking back toward the launch site.)

(5) Pitch the vehicle until the horizon is at the top of the window with earth above and sky below. (The pilot gives a hold signal to the computer operator at this time.)

(6) Hold this position until aerodynamic capture when the horizon is forced out of the field of view at the top of the window.

This procedure, which was used for all the runs performed in the simulation study, varied only in the manner in which the heading was determined. The available heading reference depended on the visual scene presented to the pilot. Landmarks in the clear scene of Florida were used for heading determination. Minimum yaw error was accomplished when either Cape Kennedy or the Tampa Bay area was used as a yaw reference. Both landmarks lay along the initial orbital track of the vehicle. Figure 11 shows the pilot's view through the docking window when using the Cape Kennedy area as a heading reference.

Heading determination when the 90-percent-cloud-cover transparencies were used required the pilot to perform a tracking task. The pilot would point the nose of the vehicle toward the earth so that he could view a complete broken-cloud-cover scene in his docking window. He would observe the motion of the cloud patterns and maneuver the vehicle until the direction of motion was parallel to the XZ-reference plane and the cloud patterns moved from top to bottom in the window. The pilot would then pitch the vehicle in the direction of the cloud motion (pitch down if the direction of motion was from top to bottom of the window) until the horizon was at the top of the window.

One of the Apollo mission requirements is that launches may be initiated under any weather conditions at any time of day. A suggested heading reference for conditions in which landmark recognition and/or tracking is impossible was the use of a payload vapor trail. The release of sodium vapor from the payload of a solid-propellant rocket such as a Nike-Cajun could produce a vapor trail. The rocket could be launched from the Cape Kennedy area at a small inclination angle to the local vertical or from the west coast of Florida over the Gulf of Mexico. In the simulation, the vapor trail was assumed to be released at an altitude between 80 000 and 100 000 feet (24 384 and 30 480 m) and was assumed to continue to an altitude of 300 000 feet (91 440 m). The sodium vapor can be used for day launches only because this vapor trail requires reflected sunlight for illumination. Trimethyl aluminum, which produces its own illumination from a chemical

reaction, can be used in the same launch vehicle for night launches. The pilot orientation procedure when the vapor trail was used as a reference was to scan the horizon through his docking window until the trail came into view (at which time the proper heading was attained). The proper roll attitude was reached when the horizon was at the top of the window and the vapor trail extended downward. The vapor trail yaw reference offered one advantage over the landmarks in that the pilot was positive of his heading when he sighted the trail.

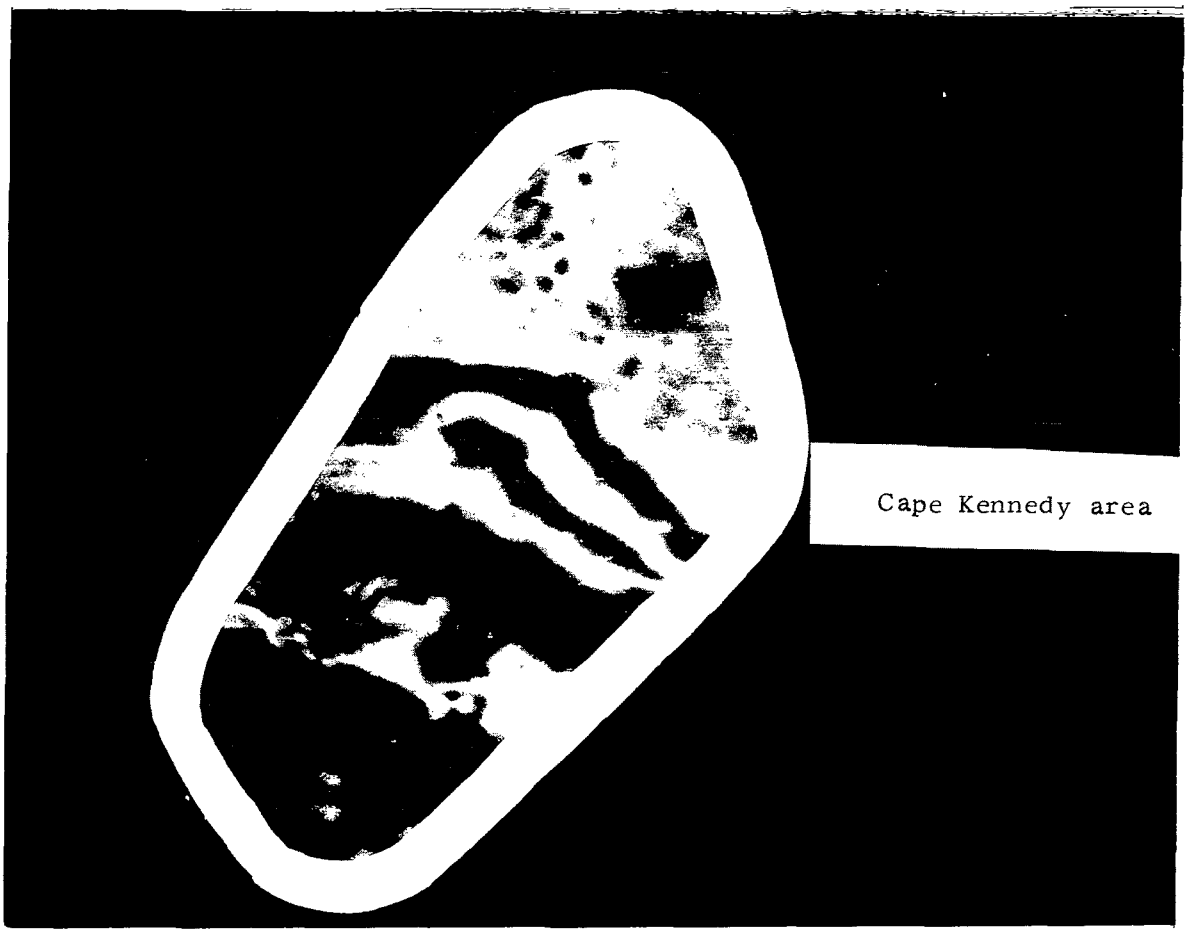

Figure 11.- Pilot's view through docking window when using Cape Kennedy area for proper heading reference. L-66-1104

Another orientation reference used by the pilots was the motion of the horizon in the window caused by aerodynamic forces acting on the vehicle. This orientation method was an outgrowth of the results obtained in the tracking maneuvers.

Eleven test pilots, including pilots from the Langley Research Center, the Manned Spacecraft Center, North American Aviation, Inc., and astronauts from the Manned Spacecraft Center participated in the study. Four of these pilots had previous experience

in reentry and launch abort simulations (using instrument displays only) and had extensive experience in RCS failure detection and correction. Most of the failure-simulation runs employed these four pilots as subjects. All the pilots performed a series of training runs prior to the data runs.

In one series of data runs, the pilot wore an unpressurized prototype Gemini pressure suit to determine whether the helmet with the visor closed would hinder his vision. The data from these runs are included with the results.

ERROR IN DEFINED PILOT PROCEDURE

The attitude orientation of the command module is accomplished by the pilot by lining up landmarks and the horizon in the docking window. The proper yaw attitude is obtained by positioning the landmarks, the vapor trail, or the motion of the cloud pattern along a line on the docking window parallel to the XZ-axis. Leveling the horizon in the docking window so that it is perpendicular to the XZ-axis produces the proper vehicle roll attitude. The proper pitch attitude, as defined in the study, exists when the horizon is at the top of the window. The pitch angle required for a heat-shield-forward trim is dependent on the angle of attack for trim and the flight-path angle of the vehicle. In the cases studied, the pitch-trim attitude required the vehicle to be oriented so that the pilot was looking up at the sky (with no natural attitude reference in his window field of view). Therefore, when the horizon is positioned at the top of the window, an error exists between the controlled angle of attack of the spacecraft and the desired angle for trim. Figure 12 shows a diagram of the vehicle orientation if the roll and yaw attitudes of the spacecraft are zero. In this figure, θ is the vehicle pitch attitude with respect to zero; B is the angle between the top of the field of view (top of window) and the X-axis of the vehicle; C is the depression angle of the horizon, which is a function of vehicle altitude; α is the vehicle angle of attack; and γ is the vehicle flight-path angle.

The depression angle of the horizon C and the vehicle flight-path angle γ are functions of the vehicle trajectory, and the angle of attack (for zero roll and yaw) is the sum of θ and γ. Therefore, for the four trajectories studied, the error in pitch attitude caused by using the horizon at the top of the window can be defined at the aerodynamic capture point.

The altitude at which capture occurs varies between 150 000 and 200 000 feet (45 720 and 60 960 m) for the four trajectories studied. The depression angle of the horizon thus varies between 7° and 8°. The field of view above the X-axis of the vehicle was 42° for the window configuration used. Therefore, for a value of C of 8° and B of 42°, when the horizon is at the top of the window, the value of θ is 146°. For the four trajectories, the value of γ varies from -5.2° for the single-control-system Saturn V

120 000-foot-altitude (36 576-m) aborts to -29.6° for the S-IB dual-control-system 150 000-foot-altitude (45 720-m) aborts. Therefore, the angle of attack varies from 151.2° to 175.6°.

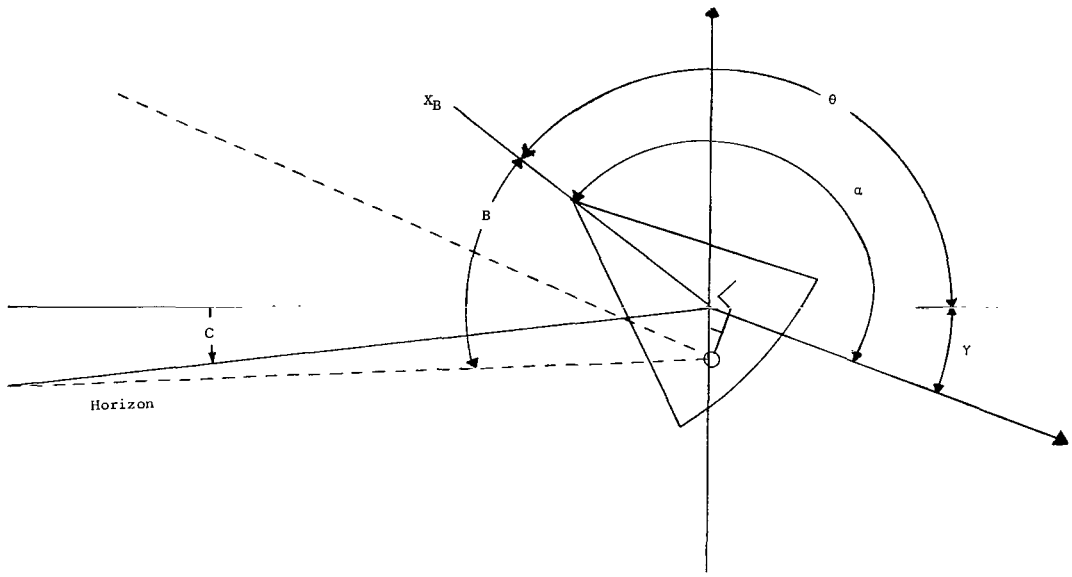

Figure 12.- Angular relations between line of sight, horizon, and vehicle direction of flight.

When the flight-path angle is between 125° and 210°, the aerodynamic forces which act on the vehicle tend to trim the vehicle toward a heat-shield-forward attitude. Thus, the top of the docking window can safely be used as a reference for reentry pitch-angle determination. With respect to yaw direction, the capture boundaries are approximately ±40° about zero.

RESULTS AND DISCUSSION

Table III gives the control time allotted to the pilot for performing the orientation maneuver in the simulation and the time which would be available in actual flight for the four abort trajectories studied. The actual time is equal to the time from abort initiation until the aerodynamic moments acting on the vehicle exceed the spacecraft control power minus the time allotted for the automatic control system to damp tumble rates of 100° per second about each axis. Spacecraft control power was considered ineffective at dynamic-pressure values above 20 lbf/ft^2 (958 N/m^2) for dual-control system operation and 10 lbf/ft^2 (479 N/m^2) for single-control-system operation. Also shown in the table are the control time and fuel required to arrest the tumbling of the spacecraft and the minimum value of the dynamic pressure during the control phase.

TABLE III.- CONTROL TIME AVAILABLE FOR REACTION CONTROL SYSTEM CONTROL OF VEHICLE ATTITUDE

Launch vehicle	Altitude,		Time required for RCS to arrest tumbling rate of 100° per sec, sec	Fuel required by RCS to arrest tumbling rates,		Control time available, sec		Minimum dynamic pressure,	
	ft	m		lbm	kg	Actual conditions	Simulation	lbf/ft^2	N/M^2
Single RCS system									
Saturn V	120 000	36 576	26.0	18.5	8.4	18	18	9.6	4.6
Saturn IB	120 000	36 576	24.5	17.0	7.7	81	77	3.3	1.6
Saturn V	150 000	45 720	27.0	17.5	7.9	133	131	.2	.1
Saturn IB	150 000	45 720	23.0	15.5	7.0	156	150	0	0
Dual RCS system									
Saturn V	120 000	36 576	12.0	19.5	8.8	70	57	9.6	4.6
Saturn IB	120 000	36 576	13.0	18.0	8.2	104	79	3.3	1.6
Saturn V	150 000	45 720	13.5	17.0	7.7	155	140	.2	.1
Saturn IB	150 000	45 720	14.0	16.0	7.3	173	158	0	0

The abort trajectories are listed in the order of increasing control time available and control authority. The most severe condition is the Saturn V 120 000-foot-altitude (36 576-m) abort with single-control-system operation. Although four abort trajectories were simulated, most of the data runs were performed by using the 120 000-foot-altitude (36 576-m) aborts because the conditions of the aborts at this altitude were more severe than those for the higher altitudes. However, the feasibility of pilot control during the lower altitude aborts indicates that pilot control would also be possible during the aborts with less severe conditions.

Control Systems

In the early phase of the study, the pilots were requested to perform half the data runs with the stabilization-and-control-system (SCS) entry control mode and half with the monitor control mode. No appreciable differences between the results for the two modes were noted. However, the pilots preferred the tighter rate dead band of the monitor mode, and this dead band was necessary for ground tracking. The remainder of the study, therefore, was conducted by using only the monitor control mode. The monitor mode had been recommended for use in the orientation maneuver by previously conducted instrument studies, and no problems which would change this recommendation were encountered in this visual study.

Test Results

Clear view of Florida.- The results of the data runs in which the clear view of Florida was used as an attitude reference are given in table IV. The data show that from

90 to 98 percent of the runs were successful when no control-system failures were investigated. The pilots who had more experience with the Apollo vehicle and participated in earlier instrument abort studies performed all runs successfully. Saturn V 120 000-foot-altitude (36 576-m) aborts with only single-control-system operation were not possible because the low control power and the short period of control time available made a landmark search impossible.

TABLE IV.- TEST RESULTS FOR CLEAR VIEW OF FLORIDA

[h = 120 000 ft (37 576 m)]

Launch vehicle	Control system	Number of runs	Success, percent	Average time, sec	Standard deviation in time, sec	Average fuel, (a)		Standard deviation in fuel, (a)	
						lbm	kg	lbm	kg
No failures									
Saturn V	Dual	79	90.2	50.0	17.8				
Saturn IB	Single	107	96.3	66.3	15.0	22.1	8.2	9.2	3.4
Saturn IB	Dual	109	98.2	48.3	20.0				
Failures inserted during runs									
Saturn IB	Single	104	79.8	73.7	16.8	25.1	9.4	10.1	3.8
Failures inserted prior to runs									
Saturn V	Dual	13	84.6	66.0	14.3				
Saturn IB	Dual	76	82.9	61.1	16.3				

[a]Blank space indicates that values were not recorded.

The runs in which control-system failures were simulated showed about 10 percent fewer heat-shield-forward captures than those with no simulated failures. All the pilots who participated in the study were unable to orient the vehicle into a heat-shield-forward attitude in at least one run. Failure was detected and corrective action was readily accomplished if the failure occurred at a time when a land view appeared in the pilot's window. However, if the failure occurred when only dark sky was visible, proper corrective action could not be initiated until some scene appeared in the window, and this loss of valuable time could have caused unsuccessful completion of the run.

There is very little difference between the results for a failure inserted prior to a run and those for a failure introduced during a run. Switching-amplifier-open malfunctions were introduced prior to a run; they caused the vehicle to continue tumbling in the failed axis after the tumbling in the other two axes had been arrested.

Rate-gyro-open failures inserted prior to a run were not simulated and therefore the pilot could always use the rate instrument to stop the tumbling. Rate-gyro-closed or switching-amplifier-closed failures inserted before the pilot took control were not

investigated because this type of failure would have caused extremely high rates which the pilot would not have been able to arrest in the available time period.

A complete familiarity with Florida landmarks and their locations with respect to each other was necessary for successful alinement of the vehicle when this scene was used as a reference. The more useful landmarks were Cape Kennedy, the Tampa Bay area, Lake Okeechobee, and the Florida Keys. The visual scene presented was an artist's conception, and the entire Florida peninsula was completely clear. Although the presented scene was considered very realistic, comparison of the scene with the view seen in actual flight could not be made because photographs of Florida from a 160 000-foot (48 768-m) altitude were not available.

Ninety-percent-cloud-cover scene with vapor trail.- Table V gives the results of the simulation runs in which the vapor trail was used as a reference; no landmarks were visible for orientation reference. However, a yaw reference was supplied by simulating a vapor trail, which extended upward from below the western horizon, in line with the spacecraft orbital track. The initial maneuver was to pitch the vehicle up until the horizon appeared in the window (if it was not already visible). The vehicle was then positioned so that the horizon was either vertical or level in the window. Then a search of the horizon was made by yawing (horizon level in window) or pitching (horizon vertical in window) the vehicle until the vapor trail came into view.

TABLE V.- TEST RESULTS FOR 90-PERCENT-CLOUD-COVER SCENE WITH VAPOR TRAIL

[h = 120 000 ft (36 576 m)]

Launch vehicle	Control system	Number of runs	Success, percent	Average time, sec	Standard deviation in time, sec	Average fuel,		Standard deviation in fuel,	
						lbm	kg	lbm	kg
No failures inserted									
Saturn V	Dual	52	90.4	56.5	18.1	35.9	16.3	16.2	7.3
Saturn IB	Single	57	96.5	69.9	18.6	20.3	9.2	9.2	4.2
Failures inserted during runs									
Saturn V	Dual	50	78.0	66.3	13.2	39.6	18.0	14.9	6.8
Saturn IB	Single	60	83.3	76.4	19.3	21.5	9.8	9.8	4.4
Pressure suit; no failures inserted									
Saturn V	Dual	19	100	62.3	15.1	35.7	16.2	14.9	6.8
Saturn IB	Single	18	100	65.8	23.3	18.9	8.6	11.9	5.4
Pressure suit; failures inserted during runs									
Saturn V	Dual	21	85.7	63.7	14.9	36.2	16.4	15.4	7.0
Saturn IB	Single	19	95	73.5	22.0	21.0	9.5	9.7	4.4

This technique had about the same results as those in which the land scene was used as a reference. Again, with no control-system failures, certain pilots had all successful data runs. Control-system failures caused about a 12-percent drop in the number of successful runs. Investigation of the single-control-system Saturn V 120 000-foot-altitude (36 576-m) aborts was not possible because of insufficient time to search the horizon. Using the vapor trail as a reference was somewhat more difficult than using the land scene because there was only one orientation reference instead of many recognizable landmarks. However, the vapor trail offered the advantage that a yaw reference was still available after final orientation; no yaw reference was available when the land scene was used. The results of runs performed by one pilot in an unpressurized prototype Gemini pressure suit are shown at the bottom of table V. The results indicate that there is no apparent impairment of vision by the closed-visor pressure-suit helmet.

Scene with no visible landmarks.- The test results for the 90-percent-cloud-cover scene with no recognizable landmarks are shown in table VI. Orientation for this case involved the establishment of a ground track for heading determination by lining up the direction of the motion of irregular cloud patterns. This maneuver required that the nose of the vehicle be pointed toward the center of the earth so that the pilot's line of vision would be perpendicular to the surface of the earth. At this attitude the highest apparent rate of motion for tracking is obtained. The rate of motion for the four trajectories investigated varied from 0.75^{o} per second to 1.5^{o} per second.

TABLE VI.- TEST RESULTS FOR 90-PERCENT-CLOUD-COVER SCENE

Launch vehicle	Altitude,		Control system	Number of runs	Success, percent	Average time, sec	Standard deviation in time, sec	Average fuel,		Standard deviation in fuel,		Comments
	ft	m						lbm	kg	lbm	kg	
Saturn IB	120 000	36 576	Single	22	81.8	80.7	16.7	26.5	12.0	7.1	3.2	Track
Saturn IB	120 000	36 576	Dual	20	70.0	99.5	6.7					Track
Saturn V	150 000	45 720	Single	26	76.9	120.2	24.7	26.6	12.1	8.0	3.6	Track
Saturn IB	150 000	45 720	Single	52	61.6	147.9	32.3	40.9	18.5	17.1	7.8	Track
Saturn V	150 000	45 720	Single	56	91.1	130.5	16.0	28.8	13.0	7.0	11.0	Track and aero trim
Saturn V	120 000	36 576	Dual	62	96.8	67.2	10.4	45.8	20.8	13.7	6.2	Aero and track
Saturn V	120 000	36 576	Single	34	97.1	65.8	12.9	22.5	10.2	7.5	3.4	Aero and track

An initial investigation of this orientation technique was conducted for the single-control-system Saturn IB 120 000-foot-altitude (36 576-m) aborts. Twenty-two runs were conducted, and four ended with apex-forward captures. This result indicated that insufficient time was available for tracking accurately enough to assure heat-shield-forward capture. Therefore, three sets of data runs were conducted, each successive

set having less severe conditions in order to allow more time for tracking. The results continued to be poor. The Saturn IB 150 000-foot-altitude (45 720-m) abort, which was the least severe condition, had only 61.6 percent successful runs. Investigation of the records and discussion with the pilots indicated that tracking was possible but not extremely accurate because of the low rate of motion of the visual scene and the small amount of time available. However, some erratic operation of the film drive system was encountered. This malfunction could have contributed to the high percentage of unsuccessful runs. In actual flight a more definite drift indication may be available to the pilot.

The highest degree of success was obtained for the single-control-system Saturn IB 120 000-foot-altitude (36 576-m) aborts; 82 percent of these aborts ended successfully. This degree of success is due mainly to the low level of control power, which can be explained by the method used for orientation. The pilot would establish a ground track and then pitch the vehicle nose to the horizon in the direction of the track motion. In the presence of a high aerodynamic field (lower altitude aborts) and a low level of vehicle control power, the aerodynamic forces would tend to trim the vehicle toward a zero yaw attitude. In other words, the aerodynamic forces would tend to remove the tracking error (yaw) as the vehicle was pitched. However, in the presence of a low aerodynamic field, the vehicle control system would overcome the low aerodynamic forces and therefore the tracking error would still exist after the vehicle had been pitched to the final attitude. If this error was greater than the capture boundary (30^{o} to 40^{o}), then when the dynamic pressure did reach a level to overcome the control system, the aerodynamic forces would flip the vehicle to an apex-forward capture. The data show that in most cases the pilot tracked the motion correctly but not accurately and thus the vehicle flipped to an apex-forward capture.

The pilots developed a technique to overcome this yaw error, designated herein as "aero trim." The method involved tracking the motion and then pitching to the horizon; when the horizon appeared in the window, the pilot would disable the spacecraft yaw and roll axes in order that the low-level aerodynamic forces could drive the vehicle in the yaw direction. (The roll axis was disabled to eliminate yaw motions caused by the roll-yaw cross-couple effects.) The yaw rate was allowed to reach about 2^{o} per second before it was damped. This procedure was repeated until either a reversal of direction occurred (indicating that the trim point had been passed) or a large angle (30^{o} to 40^{o}) was traversed. The latter indicated that a large error existed in the tracking and the vehicle was moving toward an apex-forward capture. If the vehicle had traversed a large angle, the pilot would yaw the vehicle in the opposite direction a greater amount than had been traversed and again disable the yaw axis to obtain trim if time permitted. Fifty-six runs were performed with only five losses for the 150 000-foot-altitude (45 720-m) Saturn V aborts.

These results constituted an improvement of about 15 percent over data runs at the same conditions when the aero-trim technique was not used. Although not perfect, these results did indicate that a knowledge of the aerodynamic moments acting on the vehicle could be a valuable tool in controlling the vehicle.

The tracking method of heading determination is unattractive both because of the difficulty of obtaining an accurate heading and because of the necessity of pointing the vehicle toward the earth to accomplish this task. The spacecraft in this position is vulnerable in that this vehicle attitude is conducive to apex-forward capture if the dynamic pressure buildup should occur before tracking has been completed.

Sufficient time or control power for ground tracking was not available for Saturn V 120 000-foot-altitude (36 576-m) aborts. The dynamic pressure remained relatively high throughout the runs and had a minimum of 9 lbf/sq ft (431 N/m^2). These high aerodynamic forces tended to stabilize the vehicle after tumbling at or near one of the two stable trim points. In the majority of the runs, the spacecraft stabilized near the apex-forward trim point since it was the stronger of the two trim points. The experience gained by using the aero-trim technique for yaw lineup indicated the possibility of using the motion of the vehicle caused by aerodynamic moments to determine the trim point at which the vehicle had been arrested.

The procedure was to pitch the vehicle to the horizon, if it was not already visible, and roll the vehicle (if necessary) so that the earth was at the top of the window and the sky at the bottom. The roll and yaw axes were then disabled briefly so that the vehicle could seek a yaw trim. The roll and yaw axes were then reenabled and the pitch axis was disabled so that the motion of the vehicle with respect to the horizon in the pitch direction could be monitored. If the vehicle nose moved away from the horizon (horizon moved toward the top of the window), a heat-shield-forward trim was assumed and the pitch axis was reenabled. Motion of the nose toward the horizon indicated an apex-forward trim; in this instance an immediate full pitchup maneuver was performed to bring the vehicle over to the opposite horizon near a heat-shield-forward trim. This method of control was used to perform data runs for the Saturn V 120 000-foot-altitude (36 576-m) aborts for both single- and dual-control-system operation. For the dual-control system, only 2 of 62 runs were unsuccessful, and for the single-control system, only 1 of 34 runs was unsuccessful. These results indicate that the use of aerodynamic moments acting on the vehicle is a satisfactory method for orientation for the low-altitude aborts. This method, however, may not be operationally satisfactory. The very nature of the technique requires that the dynamic pressure be at a sufficiently high level to drive the vehicle and therefore loss of vehicle control power will occur quickly. In the three unsuccessful runs, the pilots realized that they were at an apex-forward attitude, but they did not have sufficient control to maneuver the vehicle to a heat-shield-forward

attitude. Many of the successful runs required a "rocking" of the vehicle to perform the pitchup maneuver and 1 to 2 seconds delay in decision making could have caused many more unsuccessful runs.

Failures in the reaction control system were not investigated for the scene with no recognizable landmarks. It was apparent that loss of rate damping during the tracking phase would have precluded the possibility of determining track direction.

Failure Analysis

The results of the reaction-control-system-failure investigation are presented in tables VII and VIII. The switching-amplifier-closed or gyro-closed failures caused continuous full thrust in the failed axis; thus this type of failure was the most critical,

TABLE VII.- FAILURE ANALYSIS FOR CLEAR VIEW OF FLORIDA

[h = 120 000 ft (36 576 m)]

Axis	Number of runs	Number of unsuccessful runs	Average time, sec	Average fuel, lbm	Average fuel, kg	Launch vehicle	Control system
Switching amplifier open							
ψ	3	0	88.5	64.6	29.3	Saturn V	Dual
θ	5	1	82.4	29.6	13.4	Saturn V	Dual
φ	5	1	83.0	54.0	24.5	Saturn V	Dual
ψ	9	1	87.4	28.6	13.0	Saturn IB	Single
θ	6	0	63.4	19.4	8.8	Saturn IB	Single
φ	8	1	70.4	21.7	9.8	Saturn IB	Single
ψ	23	2	82.0	54.0	24.5	Saturn IB	Dual
θ	22	4	74.3	27.8	12.6	Saturn IB	Dual
φ	31	7	82.3	35.0	15.9	Saturn IB	Dual
Switching amplifier closed							
ψ	10	2	69.5	21.5	9.8	Saturn IB	Single
θ	7	3	81.3	29.1	13.2	Saturn IB	Single
φ	10	1	76.0	26.9	12.2	Saturn IB	Single
Rate gyro open							
ψ	7	1	69.3	22.4	10.2	Saturn IB	Single
θ	7	2	76.3	24.3	11.0	Saturn IB	Single
φ	8	1	76.1	28.8	13.1	Saturn IB	Single
Rate gyro closed							
ψ	9	4	69.6	24.9	11.3	Saturn IB	Single
θ	7	2	73.7	25.3	11.5	Saturn IB	Single
φ	8	2	80.8	29.9	13.6	Saturn IB	Single

especially if the pilot was looking at the sky and had no visual reference when the failure occurred. The failure could be detected only by observing the rate indicator, and the pilot's attention was directed not at the instrument but toward the out-the-window view during this search phase. Therefore, this type of failure was not readily detected and, when detected, required the pilot to stabilize the vehicle again and then to resume the orientation maneuver. The loss of valuable time often meant that the pilot was unable to orient the vehicle in the proper direction.

TABLE VIII.- FAILURE ANALYSIS FOR 90-PERCENT-CLOUD-COVER SCENE WITH VAPOR TRAIL

[h = 120 000 ft (36 576 m)]

Axis	Number of runs	Number of unsuccessful runs	Average time, sec	Average fuel,		Launch vehicle	Control system
				lbm	kg		
Switching amplifier open							
ψ	3	0	58.0	28.6	13.0	Saturn V	Dual
θ	5	1	78.8	58.0	26.3	Saturn V	Dual
φ	4	1	73.2	46.9	21.3	Saturn V	Dual
ψ	6	0	68.8	14.8	6.7	Saturn IB	Single
θ	5	3	99.5	29.4	13.3	Saturn IB	Single
φ	5	1	67.5	14.3	6.5	Saturn IB	Single
Switching amplifier closed							
ψ	6	3	72.7	41.0	18.6	Saturn V	Dual
θ	4	2	75.1	45.5	20.6	Saturn V	Dual
φ	4	1	48.0	19.7	8.9	Saturn V	Dual
ψ	4	0	63.3	17.4	7.9	Saturn IB	Single
θ	4	1	73.5	20.1	9.1	Saturn IB	Single
φ	2	1	79.1	23.4	10.6	Saturn IB	Single
Rate gyro open							
ψ	4	0	58.5	33.3	15.1	Saturn V	Dual
θ	4	1	77.1	53.7	24.4	Saturn V	Dual
φ	5	1	57.1	27.7	12.6	Saturn V	Dual
ψ	6	1	80.3	22.4	10.2	Saturn IB	Single
θ	8	1	72.3	21.3	9.7	Saturn IB	Single
φ	5	2	80.4	22.8	10.3	Saturn IB	Single
Rate gyro closed							
ψ	3	0	72.2	45.4	20.6	Saturn V	Dual
θ	4	0	62.3	33.8	15.3	Saturn V	Dual
φ	4	1	63.3	39.7	18.0	Saturn V	Dual
ψ	5	1	83.4	27.3	12.4	Saturn IB	Single
θ	4	3	65.6	19.0	8.6	Saturn IB	Single
φ	6	2	87.7	30.9	14.0	Saturn IB	Single

Fuel Usage

The available fuel for the abort maneuver is 185 pounds (84 kg) for dual-control-system operation and 72.5 pounds (33 kg) for single-control-system operation. The average amount of fuel used and the standard deviation are given for each condition in tables IV to VI. The maximum amount used for dual-control-system operation was 84 pounds (38 kg). The single-control-system operation maximum amount was 67 pounds (30 kg) for one run; the next highest amount used was 50 pounds (23 kg). These maximum fuel consumptions and those listed in tables IV to VI do not include the fuel required to stop the tumbling prior to the orientation maneuver. In order to compare the total amount of fuel used with the available amount of fuel, the fuel required to arrest the tumble rates must be added to the amounts given. The average amount of fuel used to arrest the tumbling at 100° per second is given in table III.

It should be noted that the study was a single-pilot simulation. In the actual flight, the right-hand pilot could aid greatly in the search and orientation task. Possible pilot disorientation or blackout caused by the high tumbling rates encountered prior to tower jettison was not accounted for in the simulation. The possible use of the sun position as an orientation aid was not investigated. The amount of detail and contrast level of the clear scene of Florida used in the simulation was not confirmed.

CONCLUSIONS

A fixed-base simulation study has been conducted to determine whether a pilot could manually orient the Apollo vehicle to the proper reentry attitude following a high-altitude (120 000-foot (36 576-m) and above) abort from earth launch by using only the "out-the-window" visual scene as an attitude reference. The results indicate the following conclusions:

1. If a visual yaw reference is available, such as a landmark or a vapor trail, manual orientation is possible for all aborts above a 120 000-foot altitude except the single-control-system Saturn V 120 000-foot (36 576-m) abort.

2. Heading determination by using ground tracking, which requires a broken cloud cover along the orbital track, appears feasible for aborts above a 150 000-foot (45 720-m) altitude. This technique is not usable for 120 000-foot (36 576-m) aborts because of insufficient control time for accurate ground tracking. The vulnerable spacecraft attitude required to perform the tracking task should be considered prior to adoption of this technique.

3. Knowledge of the reaction of the vehicle to aerodynamic forces can be a useful aid in determining proper vehicle orientation. However, reliance on only this knowledge for an operational orientation is not recommended.

4. Control-system failures which occur during the visually controlled abort maneuver greatly affect the pilot's ability to orient the vehicle to the heat-shield-forward attitude.

5. The amount of fuel available is sufficient for stabilization and orientation.

6. An unpressurized pressure suit does not affect the pilot's ability to perform the orientation maneuvers.

7. No operation method has been developed for the pilot using the out-the-window view to control the vehicle for the 120 000-foot (36 576-m) altitude abort from the Saturn V vehicle if only the single-control system is operational.

Langley Research Center,
National Aeronautics and Space Administration,
Langley Station, Hampton, Va., February 10, 1966.

APPENDIX

EQUATIONS

The Apollo abort study was a three-degree-of-rotation simulation in which only angular rates and positions of the vehicle were involved. However, the angular motion of the visually displayed land mass, as would be seen by an astronaut traveling down range, was programed into the simulation. Thus all motions except the lateral and vertical motions in the visual display were included in the simulation. During an abort, lateral motions would be small. The vertical motion, which would create either a growth (descending altitude) or dwarfing (ascending altitude) of the objects in the display was assumed to be negligible.

If $s = h\Omega$, h being altitude and Ω being an angle in radians about the local vertical, the tangential orbital velocity V is given as:

$$V = \dot{s} = h\dot{\Omega} + \Omega\dot{h}$$

If $\dot{h} = 0$, as assumed in the study,

$$\omega = \dot{\Omega} = \frac{V}{h}$$

The orientation of the spacecraft in the body-axis system $(X_B,\ Y_B,\ Z_B)$ can be expressed in terms of the inertial axis system $(X_i,\ Y_i,\ Z_i)$ by means of the following orthogonal-transformation matrix of quaternion numbers (ref. 2):

$$\left[E\right] = (e_{ij}) = \begin{bmatrix} a^2 - b^2 - c^2 + d^2 & 2(ab + cd) & 2(bd - ac) \\ 2(cd - ab) & a^2 - b^2 + c^2 - d^2 & 2(bc - ad) \\ 2(ac + bd) & 2(bc - ad) & a^2 + b^2 - c^2 - d^2 \end{bmatrix} \tag{1}$$

or

$$\begin{bmatrix} X_B \\ Y_B \\ Z_B \end{bmatrix} = (e_{ij})_{3X3} \begin{bmatrix} X_i \\ Y_i \\ Z_i \end{bmatrix}$$

In terms of the gimbal drive system, which had an order of rotation of yaw, pitch, and roll, the above matrix is identically equal to the matirx

$$\begin{bmatrix} \cos\psi\cos\theta & \cos\theta\sin\psi & -\sin\theta \\ \sin\theta\sin\varphi\cos\psi - \sin\psi\cos\varphi & \cos\psi\cos\varphi + \sin\theta\sin\psi\sin\varphi & \sin\varphi\cos\theta \\ \sin\theta\cos\varphi\cos\psi + \sin\psi\sin\varphi & \sin\theta\sin\psi\cos\varphi - \cos\psi\sin\varphi & \cos\theta\cos\varphi \end{bmatrix} \tag{2}$$

The rate equations which correspond to these matrices are given as (ref. 2)

$$\left.\begin{aligned} 2\dot{a} &= -dp - cq - br \\ 2\dot{b} &= -cp + dq + ar \\ 2\dot{c} &= bp + aq - dr \\ 2\dot{d} &= ap - bq + cr \end{aligned}\right\} \tag{3}$$

where p, q, and r are the angular velocities about the vehicle body axis and

$$\dot{\theta} = q\cos\varphi - r\sin\varphi \tag{4}$$

A requirement in the study was that rotation about each axis be unrestricted. This stipulation was accomplished by combining portions of equations (1) to (4) with the value of $\cos\theta$ obtained from integration:

$$\cos\theta = \int -\dot{\theta}\sin\theta\,dt \tag{5}$$

The method was as follows: The four quaternion rate equations (eq. (3)) were integrated to obtain the values of a, b, c, and d. Some of the elements of matrix (2) were formulated by using the following terms from matrix (1):

$$\left.\begin{aligned} e_{11} &= a^2 - b^2 - c^2 + d^2 = \cos\psi\cos\theta \\ e_{12} &= 2(ab + cd) = \sin\psi\cos\theta \\ e_{13} &= 2(bd - ac) = -\sin\theta \\ e_{23} &= 2(bc - ad) = \sin\varphi\cos\theta \\ e_{33} &= a^2 + b^2 - c^2 - d^2 = \cos\varphi\cos\theta \end{aligned}\right\} \tag{6}$$

The elements e_{11}, e_{12}, e_{23}, and e_{33} were then multiplied by the value of $\cos\theta$ obtained from equation (5). This multiplication is performed to give $\cos^2\theta$ in each element so that the sign of $\cos\theta$ does not affect the sign of the element. These

quantities were then used as inputs to "polar mode" resolvers in the computer. These resolvers solved the arctangent equations to supply the angles ψ, θ, and φ to drive the equipment.

$$\left.\begin{aligned} \tan\theta &= \frac{\sin\theta}{\cos\theta} = \frac{-e_{13}}{\int \dot{\theta}\, e_{13}\, dt} \\ \tan\varphi &= \frac{\sin\varphi\cos^2\theta}{\cos\varphi\cos^2\theta} = \frac{e_{23}\cos\theta}{e_{33}\cos\theta} \\ \tan\psi &= \frac{\sin\psi\cos^2\theta}{\cos\psi\cos^2\theta} = \frac{e_{12}\cos\theta}{e_{11}\cos\theta} \end{aligned}\right\} \qquad (7)$$

The use of these equations to drive the equipment, which had no mechanical restrictions, allowed unlimited rotation in all three axes.

Equations for the vehicle rotational accelerations about the yaw, pitch, and roll axes ($\dot{r}$, $\dot{q}$, $\dot{p}$), in which all cross products of inertia are retained because of the expected size of the spacecraft tumble rates (100° per second), are as follows:

$$\left.\begin{aligned} \dot{p} &= \frac{M_x}{I_{xx}} + \frac{I_{xy}}{I_{xx}}\dot{q} + \frac{I_{xz}}{I_{xx}}\dot{r} - \frac{I_{xy}}{I_{xx}}pr + \frac{I_{xz}}{I_{xx}}pq - \frac{\left(I_{xx} - I_{yy}\right)}{I_{xx}}qr - \frac{I_{yz}}{I_{xx}}\left(r^2 - q^2\right) \\ \dot{q} &= \frac{M_y}{I_{yy}} + \frac{I_{xy}}{I_{yy}}\dot{p} + \frac{I_{xz}}{I_{yy}}\dot{r} - \frac{\left(I_{xx} - I_{zz}\right)}{I_{yy}}pr - \frac{I_{xz}}{I_{yy}}\left(p^2 - r^2\right) + \frac{I_{xy}}{I_{yy}}qr - \frac{I_{yz}}{I_{yy}}pq \\ \dot{r} &= \frac{M_z}{I_{zz}} + \frac{I_{xz}}{I_{zz}}\dot{p} + \frac{I_{yz}}{I_{zz}}\dot{q} - \frac{\left(I_{yy} - I_{xx}\right)}{I_{zz}}pq - \frac{I_{xy}}{I_{zz}}\left(q^2 - p^2\right) - \frac{I_{xz}}{I_{zz}}qr + \frac{I_{yz}}{I_{zz}}pr \end{aligned}\right\} \qquad (8)$$

where I is the moment of inertia (subscripts refer to axes involved), and M is the moment that is given as

$$\left.\begin{aligned} M_X &= M_{x,A} + M_{x,RCS} \\ M_y &= M_{y,A} + M_{y,RCS} \\ M_Z &= M_{z,A} + M_{z,RCS} \end{aligned}\right\} \qquad (9)$$

The parameter $M_{x,A}$ is the moment due to aerodynamic forces about the X_B axis, and the parameter $M_{x,RCS}$ is the moment due to the vehicle reaction-control-jet forces about the X_B axis.

APPENDIX

Figure 13 shows the relationship of the velocity vector in the inertial coordinate system to that in the body-axis system. The corresponding aerodynamic moment equations are derived in the following paragraphs.

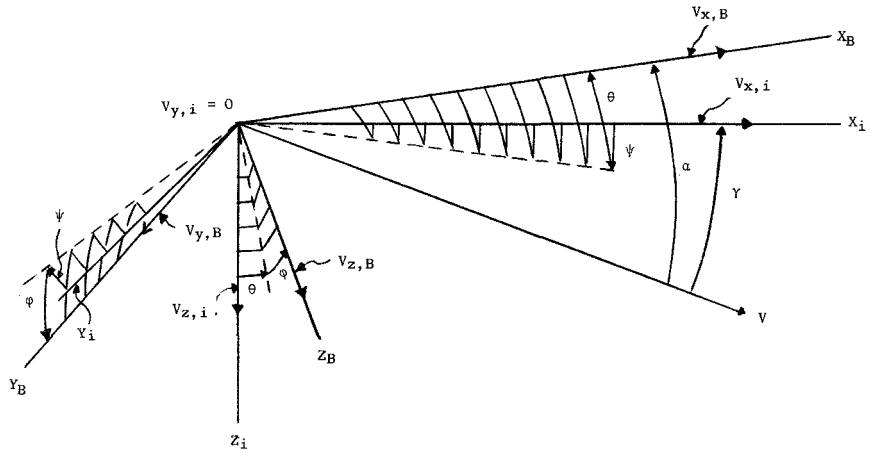

Figure 13.- Relation between inertial and body coordinate systems.

The components of the relative velocity vector V in the inertial system are:

$$\left.\begin{aligned} V_{x,i} &= V \cos \gamma \\ V_{z,i} &= V \sin \gamma \\ V_{y,i} &= 0 \end{aligned}\right\} \tag{10}$$

where γ is the relative flight-path angle measured in the X_iZ_i-plane. The components of the vector V in the body-axis system after rotation in the yaw, pitch, and roll order are:

$$\left.\begin{aligned} V_{x,B} &= V \cos \gamma \cos \psi \cos \theta + V \sin \gamma \sin \theta \\ V_{y,B} &= V \cos \gamma(\cos \psi \sin \theta \sin \varphi - \cos \varphi \sin \psi) - V \sin \gamma \cos \theta \sin \varphi \\ V_{z,B} &= V \cos \gamma(\sin \theta \cos \varphi \cos \psi + \sin \psi \sin \varphi) - V \sin \gamma \cos \theta \cos \varphi \end{aligned}\right\} \tag{11a}$$

In matrix form, these components are

APPENDIX

$$\begin{Bmatrix} V_{x,B} \\ V_{y,B} \\ V_{z,B} \end{Bmatrix} = V \begin{Bmatrix} \cos\gamma\, e_{11} - \sin\gamma\, e_{13} \\ \cos\gamma\, e_{21} - \sin\gamma\, e_{23} \\ \cos\gamma\, e_{31} - \sin\gamma\, e_{33} \end{Bmatrix} \tag{11b}$$

The angle of attack α is the angle between the velocity vector and the X_B-axis:

$$\alpha = \cos^{-1}(\cos\gamma\cos\psi\cos\theta + \sin\gamma\sin\theta) = \cos^{-1}\left(\cos\gamma\, e_{11} - \sin\gamma\, e_{13}\right) \tag{12}$$

The aerodynamic moments are given as:

$$\left.\begin{aligned} M_{x,A} &= -C_L\bar{q}S\left(Y_O - Y_{cg}\right)\cos\varphi_A + C_L\bar{q}S\left(Z_O - Z_{cg}\right)\sin\varphi_A \\ M_{y,A} &= C_m\bar{q}Sl\cos\varphi_A - C_D\bar{q}S\left(Z_O - Z_{cg}\right) + C_L\bar{q}S\left(X_O - X_{cg}\right)\cos\varphi_A \\ M_{z,A} &= -C_m\bar{q}Sl\sin\varphi_A - C_L\bar{q}S\left(X_O - X_{cg}\right)\sin\varphi_A + C_D\bar{q}S\left(Y_O - Y_{cg}\right) \end{aligned}\right\} \tag{13}$$

where S is the aerodynamic reference area; l is the aerodynamic reference length; X_{cg}, Y_{cg}, and Z_{cg} represent the center-of-gravity location with respect to the given axis; X_O, Y_O, and Z_O represent the aerodynamic center of force with respect to the given axis; and $\bar{q}$ is the dynamic pressure acting on the vehicle. The dynamic pressure $\bar{q}$ was programed for a given trajectory as a function of time from abort initiation. The aerodynamic coefficients for pitching moment C_m, lift C_L, and drag C_D are functions of the total angle of attack α.

The aerodynamic roll angle φ_A is the angle between the Z_B-axis and the component of the vector V in the Z_BY_B-plane. The sine and cosine of this angle resolve the coefficients from the α-plane into the body planes:

$$\left.\begin{aligned} \sin\varphi_A &= \frac{V_{y,B}}{\sqrt{V_{y,B}^2 + V_{z,B}^2}} = \frac{V\cos\gamma\, e_{21} - V\sin\gamma\, e_{23}}{\sqrt{\left(V\cos\gamma\, e_{21} - V\sin\gamma\, e_{23}\right)^2 + \left(V\cos\gamma\, e_{31} - V\sin\gamma\, e_{33}\right)^2}} \\ \cos\varphi_A &= \frac{V_{z,B}}{\sqrt{V_{y,B}^2 + V_{z,B}^2}} = \frac{V\cos\gamma\, e_{31} - V\sin\gamma\, e_{33}}{\sqrt{\left(V\cos\gamma\, e_{21} - V\sin\gamma\, e_{23}\right)^2 + \left(V\cos\gamma\, e_{31} - V\sin\gamma\, e_{33}\right)^2}} \end{aligned}\right\} \tag{14}$$

APPENDIX

The Apollo vehicle has 12 attitude jets which operate in cooperative pairs. Three pairs operate to produce positive-direction rotation about the X, Y, and Z axes of the vehicle. The other three pairs operate in the opposite direction to produce negative-direction rotation. For example, jets 10 and 12 operate together to produce a positive roll moment, while jets 9 and 11 operate in an opposite direction to produce a negative roll moment. In notation form,

$$\text{Roll jets } -\begin{pmatrix}9\\11\end{pmatrix}\leftrightarrow\begin{pmatrix}10\\12\end{pmatrix}+$$

In a similar manner,

$$\text{Pitch jets } -\begin{pmatrix}2\\4\end{pmatrix}\leftrightarrow\begin{pmatrix}1\\3\end{pmatrix}+$$

$$\text{Yaw jets } -\begin{pmatrix}6\\7\end{pmatrix}\leftrightarrow\begin{pmatrix}5\\8\end{pmatrix}+$$

The forces F about the X_B, Y_B, and Z_B axes produced by these jets are determined from

$$\left.\begin{aligned} F_x &= -\left[073\left(F_2 + F_4\right) + 0.23F_3 + 0.73\left(F_5 + F_6 + F_7 + F_8\right)\right] \\ F_y &= 0.68\left(F_5 + F_8 - F_6 - F_7\right) + 0.28\left(F_9 - F_{12}\right) + 0.93\left(F_{11} - F_{10}\right) \\ F_z &= F_1 + 0.68\left(F_2 + F_4\right) + 0.96\left(F_9 + F_{12}\right) + 0.975F_3 - 0.36\left(F_{10} + F_{11}\right) \\ &\quad - 0.042\left(F_5 + F_6 - F_7 - F_8\right) \end{aligned}\right\} \tag{15}$$

The constants resolve that jet force into components along the given axis. Likewise, the moments about X_B, Y_B, and Z_B due to the reaction control jets are

$$\left.\begin{aligned} M_{x,RCS,O} &= 0.545\left(F_5 - F_6 - F_7 + F_8\right) - 5.35F_{12} + 5.92F_{11} - 6.2F_{10} + 5.43F_9 \\ M_{y,RCS,O} &= -3.792F_1 + 5.66\left(F_2 + F_4\right) - 3.45F_3 + 0.62\left(F_9 + F_{12}\right) \\ &\quad - 0.23\left(F_{10} + F_{11}\right) + 0.1\left(F_5 + F_6\right) + 0.892\left(F_7 + F_8\right) \\ M_{z,RCS,O} &= 5.01\left(-F_5 + F_6 + F_7 - F_8\right) - 0.18\left(F_9 - F_{12}\right) + 0.6\left(F_{10} - F_{11}\right) \end{aligned}\right\} \tag{16}$$

where the constants represent moment arms.

From equations (15) and (16), the moments due to the reaction control jets about the X_B, Y_B, and Z_B axes are found:

$$\left.\begin{aligned} M_{x,RCS} &= M_{x,RCS,O} - F_y\left(Z_O - Z_{cg}\right) + F_z\left(Y_O - Y_{cg}\right) \\ M_{y,RCS} &= M_{y,RCS,O} + F_x\left(Z_O - Z_{cg}\right) - F_z\left(X_O - X_{cg}\right) \\ M_{z,RCS} &= M_{z,RCS,O} - F_z\left(Y_O - Y_{cg}\right) + F_y\left(X_O - X_{cg}\right) \end{aligned}\right\} \quad (17)$$

The mass of the fuel used was given by the following integration:

$$W = \int \frac{F_t}{I_{sp}}\, dt$$

where

W weight of fuel

I_{sp} specific impulse

F_t total absolute force of all jets

REFERENCES

1. Mechtly, E. A.: The International System of Units - Physical Constants and Conversion Factors. NASA SP-7012, 1964.

2. Robinson, Alfred C.: On the Use of Quaternions in Simulation of Rigid-Body Motion. WADC Tech. Rept. 58-17, U.S. Air Force, Dec. 1958. (Available From ASTIA as AD No. 234422.)

"The aeronautical and space activities of the United States shall be conducted so as to contribute . . . to the expansion of human knowledge of phenomena in the atmosphere and space. The Administration shall provide for the widest practicable and appropriate dissemination of information concerning its activities and the results thereof."

—NATIONAL AERONAUTICS AND SPACE ACT OF 1958

NASA SCIENTIFIC AND TECHNICAL PUBLICATIONS

TECHNICAL REPORTS: Scientific and technical information considered important, complete, and a lasting contribution to existing knowledge.

TECHNICAL NOTES: Information less broad in scope but nevertheless of importance as a contribution to existing knowledge.

TECHNICAL MEMORANDUMS: Information receiving limited distribution because of preliminary data, security classification, or other reasons.

CONTRACTOR REPORTS: Technical information generated in connection with a NASA contract or grant and released under NASA auspices.

TECHNICAL TRANSLATIONS: Information published in a foreign language considered to merit NASA distribution in English.

TECHNICAL REPRINTS: Information derived from NASA activities and initially published in the form of journal articles.

SPECIAL PUBLICATIONS: Information derived from or of value to NASA activities but not necessarily reporting the results of individual NASA-programmed scientific efforts. Publications include conference proceedings, monographs, data compilations, handbooks, sourcebooks, and special bibliographies.

Details on the availability of these publications may be obtained from:

SCIENTIFIC AND TECHNICAL INFORMATION DIVISION

NATIONAL AERONAUTICS AND SPACE ADMINISTRATION

Washington, D.C. 20546